Available online at www.sciencedirect.com

SCIENCE DIRECT

Bioelectrochemistry 68 (2006) 158 – 170

Bioelectrochemistry

www.elsevier.com/locate/bioelechem

Interfacial ternary complex DNA/Ca/lipids at anionic vesicle surfaces

Alina Frantescu, Katja Tönsing, Eberhard Neumann *

Physical and Biophysical Chemistry, Faculty of Chemistry, University of Bielefeld, P. O. Box 100131, D-33615 Bielefeld, Germany

Received 22 February 2005; received in revised form 3 June 2005; accepted 8 June 2005
Available online 24 August 2005

Abstract

The electroporative transfer of gene DNA and other bioactive substances into tissue cells by electric pulses gains increasing importance in the new disciplines of electrochemotherapy and electrogenetherapy. The efficiency of the electrotransfer depends crucially on the adsorption of the gene DNA and oligonucleotides to the plasma cell membranes. Here it is shown that the adsorption of larger oligonucleotides such as fragments (ca. 300 bp) of sonicated calf-thymus DNA, to anionic lipids of unilamellar vesicles (diameter $\Phi = 300 \pm 90$ nm) is greatly enhanced by divalent cations such as Ca^{2+}-ions. Applying centrifugation, bound and free DNA are monitored optically at the wavelength $\lambda = 260$ nm. Using arsenazo III as a Ca^{2+}-indicator and atomic absorption spectroscopy (AAS), Ca^{2+}-titrations of DNA and vesicles yield the individual equilibrium constants of Ca^{2+}- and DNA-binding not only for the binary complexes: Ca/lipids, Ca/DNA and DNA/lipids, respectively, but also for the various processes to form the ternary complex DNA/Ca/lipids. The data provide the basis for goal-directed optimization protocols for the adsorption and thus efficient electrotransfer of oligonucleotides and polynucleotides into cells.

Keywords: Polynucleotides; Oligonucleotides; Ca^{2+}-binding constants; Electrified membrane interface; Monolayer adsorption; Complex thermodynamics

1. Introduction

The direct electrotransfer of "naked" gene DNA and other bioactive molecules into tissue cells is of crucial interest in the new medical disciplines of electrochemotherapy and electrogenetherapy [1]. The concept and technique of membrane electroporation (MEP), introduced in 1982 [2], gains increasing functional importance in medical therapies with minimum risk of undesired side effects [1,3,4]. The efficiency of the electrotransfer of oligonucleotides [5] and polynucleotides, especially at the lower, harmless field strengths of the applied electric pulses is greatly enhanced by prior adsorption of the bioactive polyelectrolytes on the cell membrane surfaces, before the actual therapeutic pulsing.

In order to quantify DNA adsorption to electrified cell surfaces, we use anionic lipid vesicle surfaces to mimic the lipid parts of cell plasma membranes for the Ca^{2+}-dependent binding of DNA. There are many studies on the interaction between Ca^{2+}-ions and lipid vesicles with different composition of lipids in the absence of DNA [6–9] or with DNA and zwitterionic and positively charged liposomes [10,11]. Also the binding of different cations to DNA has been quantified previously [12–14]. Here, we address the thermodynamics of ternary complexes in general and the ternary complex Ca/DNA/lipid vesicles, in particular. We continue to model the lipid part of curved cell membranes by spherical unilamellar lipid vesicles, using a mixture of 1 mM PS:2POPC (VET 400) which at pH 7.4 form negatively charged lipid surfaces providing electrified interfaces. Since DNA is a negatively charged polyelectrolyte, divalent cations such as Mg^{2+} and Ca^{2+} have been traditionally used to bridge the DNA with negatively charged cell membranes [2,15,16]. The formation of ternary complexes Ca/DNA/lipids is also indicated at the interface air/solution of lipid monolayers [17].

Here these interface complexes are further quantified. In detail, using centrifugation techniques, the individual equilibrium constants of Ca^{2+}- and DNA-binding are determined not only for the binary complexes Ca/lipids,

* Corresponding author. Tel.: +49 521 106 2053; fax: +49 521 106 2981.
E-mail address: eberhard.neumann@uni-bielefeld.de (E. Neumann).

1567-5394/$ - see front matter © 2005 Elsevier B.V. All rights reserved.
doi:10.1016/j.bioelechem.2005.06.003

Ca/DNA and DNA/lipids, respectively, but also for the various processes to form the ternary complex DNA/Ca/lipids on the electrified lipid bilayer surface. The data provide chemical-compositional information for goal-directed optimization protocols for the adsorption of oligonucleotides and polynucleotides to cells, to be used for the efficient electrotransfer into cells.

2. Materials and methods

Synthetic palmitoyl-oleoyl-phosphatidylcholine (POPC) is from Lipoid GmbH (Ludwigshafen, Germany). Bovine brain extract type III (containing 80%–85% phosphatidylserine (PS)), for the monolayer experiments, and synthetic PS (98% purity) is from Sigma Chemie GmbH (Deisenhofen, Germany). Unilamellar lipid vesicles of 1 mM PS:2 POPC are prepared by the vesicle extrusion technique (VET) [18,19]. Pressing the lipid mixture 21 times through a porous (400 nm) polycarbonate membrane in a LipoFast Extruder (Avestin/Milsch, Germany) yields vesicles with diameters of 300±90 nm. In this way, the vesicle samples have been prepared for each individual total Ca^{2+} concentration $[Ca_t]$ in the suspension. To avoid osmotic pressure problems, $CaCl_2$ is added to the buffer solution before the vesicle preparation to balance $[Ca_t]$. The DNA has been added to the vesicle suspension at various $[Ca_t]$.

High polymeric deoxyribonucleates (DNA type I) from calf thymus (Sigma Chemical GmbH) have been used to obtain DNA fragments of lengths 102±17 nm or 300±50 bp (determined by gel electrophoresis) by 180 sonication cycles (à 30 s) within 90 min using an ultrasound transducer (Branson Sonic Power Company, USA).

All solutions are 1 mM HEPES, pH 7.4 buffer, $T=293$ K (20 °C). The total lipid concentration is $[L_t]=1$ mM, corresponding to a vesicle density of 6.6×10^{11} per mL buffer solution. The number of DNA molecules, for instance at the lowest concentration 35.5 μM (bp) in molar base pairs (bp), refers to $7\cdot10^{13}$ DNA molecules per mL buffer.

The centrifugations have been performed at $2.3\cdot10^5$ g, 60,000 rotations per minute for 45 min. The total concentration of DNA in the supernatant, $[D_t]^{sup}$, is determined from the absorbance A_{260} at the wavelength $\lambda=260$ nm using an UVIKON 943, double beam UV/VIS spectrophotometer (Kontron Instruments).

The sedimentation coefficient for DNA fragments of 250 bp is $s_{20,w}=11$ S. To have sedimentation, the centrifugal velocity must be at least twice as large (5×10^5 g) as the one (2.3×10^5 g) used here; see also [20,21]. Therefore, we can safely neglect contributions from sedimentation.

The Ca^{2+}-indicator arsenazo III (Ar III) (Aldrich Chemical Company Inc.) is used to determine the concentration [Ca] of free Ca^{2+} in the supernatant. A 100 μM stock solution is diluted with Ca^{2+} solutions to a final concentration of [Ar]=10 μM. The calibration curve is determined from the differences in the absorbance A_{602} at $\lambda=602$ nm (Ca^{2+}-sensitive wavelength) of these samples and a sample with 1 mM EDTA ([Ca]=0) [22].

Atomic absorption spectroscopy (AAS, PYE UNICAM SP 1900 (Philips GmbH, Kassel, Germany)) has been used to determine the total Ca^{2+} concentration in the supernatant. The calibration of the apparatus has been performed in two ranges. Standard calcium solutions have been obtained by dilution of a 1 M standard calcium stock solution. $LaCl_3$ (stock solution 10%) has been added to yield a final concentration of 1% La. The calcium content of the probe is determined by spraying aliquots of 190 μl into an air–acetylene flame and measuring the absorbance at the resonance line 422.7 nm. $LaCl_3$ has been also added to each supernatant sample (1%). A mean value from 3 measurements is used to quantify the total Ca^{2+} concentration, $[Ca_t]^{sup}$, in the supernatant.

The monolayer experiments have been carried out in a Teflon trough ($10\times24\times0.3$; cm) from Riegler and Kirstein GmbH, Potsdam, Germany. The trough is filled with 1 mM HEPES, 10 mM NaCl, pH 7.4, $T=293$ K (20 °C). The Ca^{2+} concentration is varied with $CaCl_2$ in the range $0\leq[Ca_t]/mM\leq1$. The surface pressure is measured by the Wilhelmy method. After spreading 20 μL of the mixture 1 PS:2 POPC (1 mg/mL) dissolved in *n*-hexane at the air–water interface and waiting for *n*-hexane evaporation, the surface pressure-area isotherms are recorded. In the case of 1 mM $CaCl_2$ and 35.5 μM (bp) DNA, the DNA is added together with the buffer in the sub-phase. The π/A isotherms are recorded 10 times and a mean isotherm is documented.

3. Results

3.1. Monolayer/DNA interaction

In Fig. 1, typical surface pressure/area isotherms of a lipid mixture PS:2POPC are shown. In the case of $[Ca_t]=0$, the collapse point is given by A_{coll} ($[Ca_t]=0$)=92 cm^2. At $[Ca_t]=0.5$ mM, A_{coll} ($[Ca_t]=0.5$ mM)=93 cm^2; the isotherms are almost identical. However, at $[Ca_t]=1$ mM, the collapse point is shifted to the lower value A_{coll} ($[Ca_t]=1$ mM)=82 cm^2. When 35.5 μM (bp) DNA is added into the subphase at $[Ca_t]=1$ mM the collapse area A_{coll} ($[Ca_t]=1$ mM; DNA)=97.5 cm^2 is larger than that for $[Ca_t]=0$.

3.2. Optical densities of the suspensions

As seen in Fig. 2, the optical density, OD_{365}, at the wavelength $\lambda=365$ nm of a vesicle suspension increases with increasing $[Ca_t]$. It is noted that the data points of the two documented sets refer to samples which are separately extruded at the given $[Ca_t]$-values, respectively. The data scatter within the indicated range, but they are consistent with a binding isotherm. Hence, OD_{365} will be used to determine the equilibrium constant for the binding of Ca^{2+}

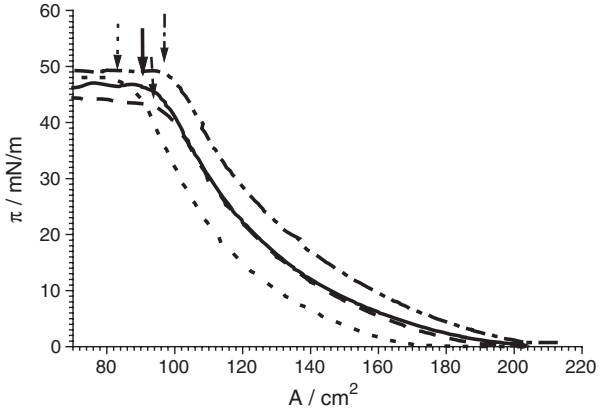

Fig. 1. Surface pressure (π)–area (A) isotherms of the lipid mixture PS:2POPC (1 mg/ml) in *n*-hexane spread at the air–water interface and sub-phases at the conditions [Ca_t]/mM=0 (—), 0.5 (--), 1 (---) without DNA and [Ca_t]=1 mM (—-) with 35.5 μM (bp) DNA, T=293 K (20 °C), 1 mM HEPES, 10 mM NaCl, pH 7.4. The arrows indicate the collapse points.

to the vesicle surface. In line with previous experience [23], aggregation of lipid vesicles starts only at [Ca_t] ≥2 mM. At our conditions of [Ca_t] ≤ mM, the turbidity (OD) data are consistent with classical binding isotherms; there is not any sign indicative for vesicle aggregation.

3.3. Ca^{2+}-binding to DNA

The absorbance A_{260} of DNA at the wavelength λ=260 nm (absorbance maximum) is traditionally used to calculate the concentration of DNA and to indicate interactions of DNA with other substances. Generally, the concentration [D] of DNA in solution is calculated from Lambert–Beer's law according to:

$$[D] = A_{260}/\varepsilon \cdot d \quad (1)$$

where d is the optical path length and ε is the absorption coefficient at λ=260 nm. In buffer solution, the absorption coefficient of the free DNA double strand is given by ε_D=13,200 M^{-1} cm^{-1}, where [D] refers to molarity of base pairs (bp). In Fig. 3, A_{260} decreases with increasing total Ca^{2+} concentration [Ca_t], starting at [Ca_t]=0, where we assume that the degree of binding is β_{CaD}=0, down to apparent saturation A_{min} referring to β_{CaD}=1, yielding ε_{CaD}=12,600 M^{-1} cm^{-1}. Note that Ca^{2+} induces aggregation of DNA fragments only at the high concentration of [Ca_t] >50 mM [24]. Thus, our condition of [Ca_t]=1 mM is far below the aggregation limit. Experimentally, the absorbance of the DNA/Ca^{2+} titration looks like a classical binding isotherm (Fig. 3). There is not any sign indicative for aggregation.

3.4. Ternary complex DNA/Ca/lipids

The Ca^{2+}-titrations of lipid vesicles in the presence of DNA of total concentration [D_t] in the suspension show that the absorbance A_{260}([D_t])=OD_{260}(Ves+[D_t])−OD_{260}(Ves) changes differently with increasing total Ca^{2+} concentration [Ca_t], see Fig. 4A. The A_{260}-values are calculated from the differences of the optical densities OD_{260}(Ves+[D_t]) in the presence of DNA and vesicles, and that in the absence of DNA, respectively. As already seen in Fig. 3, A_{260} of DNA in the absence of vesicles reflects both the complexed DNA and free DNA starting with $A_0=\varepsilon_D \cdot d \cdot [D_t]$ and heading at the saturation value $A_{min}=\varepsilon_{CaD} \cdot d \cdot [D_t]$, where all DNA is complexed; see below.

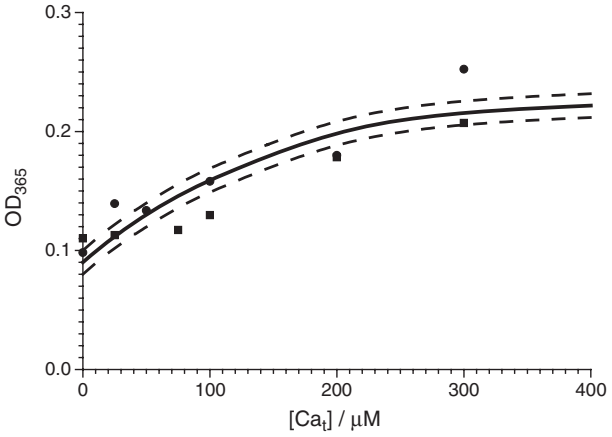

Fig. 2. Spectrophotometric (OD_{365}) Ca^{2+}-titration of two selected sets of vesicle preparations. The data of set 1(■) and set 2 (●) refer each to a given [Ca_t], respectively. The difference $\Delta OD = OD_{365} - OD^0_{365}$ is assumed to be proportional to Ca^{2+} bound [Ca_b]. The initial OD^0_{365}=0.09±0.02 refers to Ca^{2+} bound at [Ca_t]=0. The apparent maximum OD^{max}_{365}=0.23±0.02 refers to $[Ca_b]^{max}$. The dashed lines represent the data fit with Eq. (10) of the text, yielding the equilibrium constant K^0_{Ca}=15±5 μM at 1 mM HEPES, pH 7.4, T=293 K (20 °C). The full thick line represents the mean of the fitting line for the two documented, separated data sets.

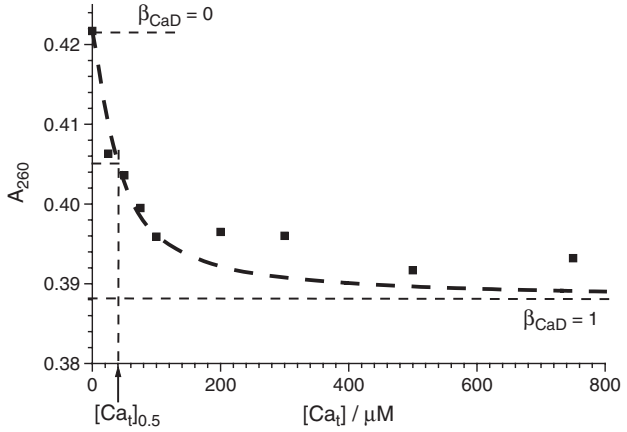

Fig. 3. Spectrophotometric (A_{260}) Ca^{2+}-titration of a DNA solution at [D_t]=32 μM (bp). Here the initial absorbance A_0=0.422±0.002 refers to the degree of Ca^{2+}-binding to DNA β_{CaD}=0. The estimated saturation value A_{min}=0.388±0.002 refers to β_{CaD}=1. The dashed line (- -) represents the data fit with Eq. (13) of the text, yielding the equilibrium constant K^0_{CaD}=24±5 μM at 1 mM HEPES, pH 7.4, T=293 K (20 °C).

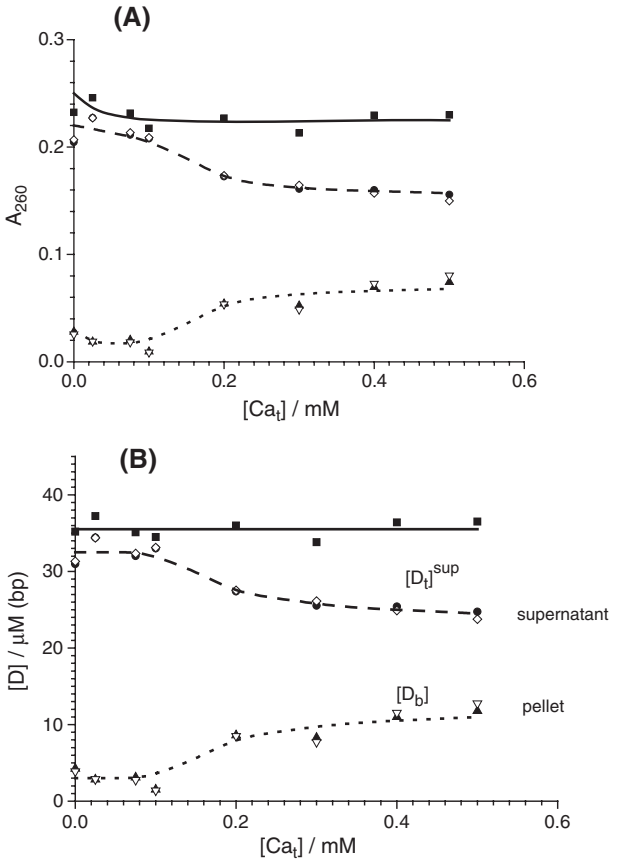

Fig. 4. Ca^{2+}-titration of the DNA/vesicle suspension at $[D_t]$=35.5 μM (bp) and of the supernatant (sup), respectively. Measured data points (A): (■) $A_{260}([D_t])=OD_{260}(Ves+[D_t])-OD_{260}(Ves)$ of the suspension; (●), (◇), $A_{260}([D_t]^{sup})$ refers to the supernatant. The values (▲), (▽) are calculated from $A_{260}([D_b])= A_{260}([D_t])-A_{260}([D_t]^{sup})$ of the pellet. Calculated $[D]$-values (B): (■), $[D_t]$ calculated with Eq. (1) of the text; (●); (◇) refer to the total DNA ($[D_t]^{sup}=[D]+[CaD]$) in the supernatant; (▲), (▽) refer to the calculated concentration ($[D_b]=[DB]+[DCaB]$) of bound DNA in the pellet. Note, that the data points at the various $[Ca_t]$ refer to aliquots of the same vesicle preparation, the supernatant data to two aliquots at a given $[Ca_t]$. T=293 K (20 °C), 1 mM HEPES, pH 7.4.

The absorbance $A_{260}([D_t]^{sup})$ of the supernatant of the centrifuged mixture of vesicles decreases after a 'delay' in the range of $0 \leq [Ca_t]/mM \leq 0.1$, tending finally to an apparent saturation value. The difference $A_{260}([D_b])= A_{260}([D_t])-A_{260}([D_t]^{sup})$ reflects the increase of bound DNA with increasing $[Ca_t]$. If higher concentrations of DNA are used, all A_{260}-values are larger, but the relative changes with increasing $[Ca_t]$ are the same as for the lowest DNA concentration with $[D_t]$=35.5 μM (bp). Using Eq. (1), the quantities A_{260} of Fig. 4A are converted to the respective concentrations: $[D_t]$ and $[D_t]^{sup}$ of Fig. 4B. Mass conservation dictates then that the bound DNA is given by:

$$[D_b] = [D_t] - [D_t]^{sup}. \quad (2)$$

In Fig. 4B, it is seen that $[D_b]$ sigmoidally (delay) increases and then appears to saturate with increasing $[Ca_t]$. Note that already at $[Ca_t]=0$, there is some DNA bound to the vesicle surface, denoted by $[D_b^0]$.

3.5. Determination of [Ca] with arsenazo III (Ar)

The Ca^{2+}-indicator arsenazo III is traditionally used for the optical indication of Ca^{2+} at the wavelength λ=602 nm [25]. Here, we apply Ar to the supernatant of the centrifuged samples. First the absorbance A_{602} of a solution of [Ar]=10 μM is measured as a function of $[Ca_t]$ to yield an optical calibration curve (data not shown). Formally, the assumption of a simple stoichiometry Ca:Ar=1:1 [22,26] is sufficient to estimate the concentration [Ca] of free Ca^{2+} according to the mass conservation:

$$[Ca] = [Ca_t] - [CaAr] = [Ca_t] - \beta_{CaAr}[Ar_t] \quad (3)$$

where the degree of Ca^{2+} bound to Ar is given by:

$$\beta_{CaAr} = \frac{[CaAr]}{[Ar_t]} = \frac{[Ca]}{[Ca]+K_{CaAr}} = \frac{\Delta A_{602}}{\Delta A_{602}^{max}} \quad (4)$$

It is readily shown that the concentration of free Ca^{2+} is given by:

$$[Ca] = \frac{1}{2}[([Ca_t] - [Ar_t] - K_{CaAr}) + X],$$
$$\text{where } X = \sqrt{([Ca_t] + [Ar_t] + K_{CaAr})^2 - 4\cdot[Ca_t]\cdot[Ar_t]}. \quad (5)$$

As expected, $[Ca]=[Ca_t]$ for a solution without DNA and without vesicles. See Fig. A1 of the Appendix.

3.6. The total Ca^{2+} concentration in the supernatant by AAS

The calibration line, A_{422} versus $[Ca_t]^{sup}$, at the resonance line for Ca^{2+}, λ=422.7 nm, is established with standard solutions containing 1% (weight) La^{3+} for the two

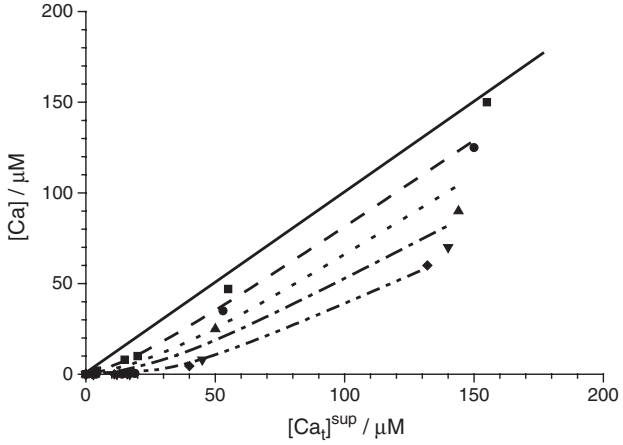

Fig. 5. Ca^{2+}-binding isotherms. [Ca] versus $[Ca_t]^{sup}=[Ca]+[CaD]$ in the supernatant of the centrifuged vesicle suspensions for different DNA concentrations: $[D_t]$/μM (bp)=(■) 0, (●) 35.5, (▲) 71, (▼) 107 and (♦) 143; from top to bottom. The data fit, using Eq. (12) of the text with $[CaD]^{max}=[D_t]^{sup}$, yields K_{CaD}^0=24±5 μM at T=293 K (20 °C), 1 mM HEPES, pH 7.4. The straight full line refers to: $[Ca]=[Ca_t]^{sup}$ at $[D_t]$=0.

concentration ranges: $0 \leq [Ca_t]/\mu M \leq 100$ and $100 \leq [Ca_t]/\mu M \leq 500$ (data not shown). The La^{3+}-ions displace Ca^{2+}-ions from the binding sites and make them available for the AAS measurements in the supernatant [27,28].

As seen in Fig. 5, at a given $[Ca_t]^{sup}$, [Ca] in the supernatant decreases with increasing amounts of DNA $[D_t]$ in the suspension. Comparisons refer to the same $[Ca_t]^{sup}$ consistent with $[Ca]=[Ca_t]^{sup}-[CaD]$. As expected, with increasing concentration of free DNA, $[D]$, in the supernatant, the concentration $[CaD]$ is also increasing. In the case of vesicle suspensions without DNA, the equality $[Ca_t]^{sup}=[Ca]$ holds (straight full line). The scatter of the data points is relatively large, because two methods are used to determine the Ca^{2+} concentration in the supernatant. $[Ca_t]^{sup}$ is measured by AAS and [Ca] is determined by using arsenazo III as an optical indicator.

4. Data evaluation and discussion

4.1. Evidence for DNA binding to a PS:2POPC lipid monolayer

As recalled from Fig. 1, the monolayer data exhibit different values for the collapse area in the π/A isotherms. The area per molecule at collapse, a_{coll}, is calculated according to:

$$a_{coll} = A_{coll}/N = A_{coll}\overline{M}/(N_A \cdot c \cdot V) \tag{6}$$

from the experimental collapse area, A_{coll}, of the lipid film. N_A is the Avogadro constant, $\overline{M}=784.06$ g/mol is the average molar mass of a lipid in the mixture of 1 PS:2 POPC, N the number of lipid molecules in the mixture, $c=1$ mg/ml the mass concentration and $V=20$ µl, the volume of the lipid solution spread on the surface. The areas per molecule occupied by the lipids are: $a_{coll}([Ca_t]=0)=0.6$ nm^2, $a_{coll}([Ca_t]=0.5$ mM$)=0.605$ nm^2 and $a_{coll}([Ca_t]=1$ mM$)=0.535$ nm^2. The quantities $a_{coll}=0.58$ nm^2 for PC and $a_{coll}=0.574$ nm^2 for PS have been obtained by NMR studies [29]. A value of 0.42 nm^2 has been found for DMPC [30].

The decrease of the area per molecule at collapse in the presence of Ca^{2+}-ions (see also Huster et al. [29]) is consistent with the binding of the divalent cations to the negatively charged groups of phosphatidylserine [31], leading to a denser packing of the lipids in the monolayer films; hence a smaller area is occupied by one lipid molecule. When DNA is added to the aqueous phase at $[Ca_t]=1$ mM, the area per molecule increases up to 0.635 nm^2, indicating DNA inserting into the lipid film. It appears that DNA binds at the lipid monolayer interface through Ca^{2+}-ions, providing indirect evidence for the ternary complex Ca/DNA/lipids.

4.2. Overall scheme for the Ca^{2+} and DNA binding reactions

Fig. 6 displays the overall scheme for the various binary complexes and the ternary complex DNA/Ca/B, where B refers to binding sites on the vesicle surface. In detail, DNA (D), Ca^{2+}-ions and the binding sites B on the surface of the vesicles form the complex D/Ca/B along different pathways. The scheme expresses all binding steps as 1:1 complexes. Note that D refers to one base pair (bp) and B to probably two charged lipid head groups (of two PS molecules).

The apparent dissociation equilibrium constants of the binary complexes are defined as:

$$K^0_{Ca} = [Ca]\cdot\frac{[B]}{[CaB]}, \quad K^0_{CaD} = [Ca]\cdot\frac{[D]}{[CaD]},$$
$$K^0_D = [D]\cdot\frac{[B]}{[DB]} \tag{7}$$

respectively. The three different ternary complex formations are characterized by:

$$K'_D = [D]\cdot\frac{[CaB]}{[DCaB]}, \quad K'_{CaD} = [CaD]\cdot\frac{[B]}{[DCaB]},$$
$$K'_{Ca} = [Ca]\cdot\frac{[DB]}{[DCaB]}. \tag{8}$$

The individual reaction steps are treated now separately.

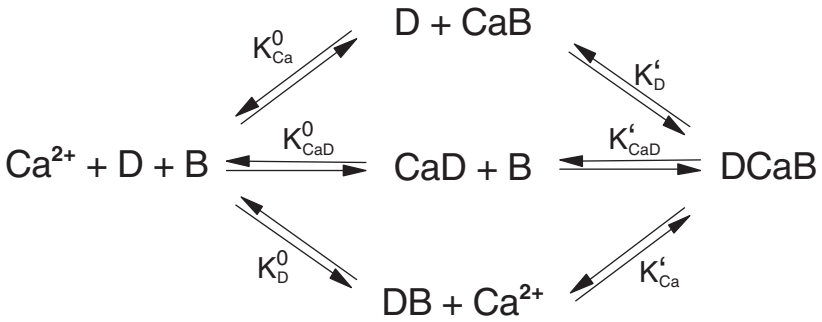

Fig. 6. Overall cyclic reaction scheme for the binding of Ca^{2+}-ions to DNA (D) and to B-sites on the lipid vesicle surface, leading to the various binary complexes and the ternary complex DCaB on the outer vesicle surface. The B-sites for the binding of DNA and Ca^{2+} are the anionic head groups of the lipids.

4.3. Ca^{2+}-binding to sites B on the vesicle surface

In the absence of DNA, the binding of Ca^{2+} to surface sites B is described by: $Ca+B \rightleftharpoons CaB$, where B represents one or more anionic lipid head groups. Written in dissociation direction, we have:

$$CaB \rightleftharpoons Ca + B \tag{9}$$

characterized by the dissociation equilibrium constant K^0_{Ca}, defined by Eq. (7). The degree of Ca^{2+}-binding, β_{Ca}, to B-sites on the vesicle surface is given by:

$$\beta_{Ca} = \frac{[Ca_b]}{[Ca_b]^{max}} = \frac{[CaB]}{[B_t]} = \frac{[Ca]}{[Ca] + K^0_{Ca}} \tag{10}$$

where $[B_t]$ is the total concentration of B-sites. The differences in the optical densities (turbidities), $\Delta OD_{365} = OD_{365} - OD^0_{365}$ and $\Delta OD^{max}_{365} = OD^{max}_{365} - OD^0_{365}$ (Fig. 2), where OD^0_{365} refers to $[Ca_t]=0$, are used to determine $\beta_{Ca} = \Delta OD / \Delta OD^{max}$. In Eq. (10), $[Ca_b]$ is the concentration of bound Ca^{2+} in the pellet, $[Ca_b]^{max}$ is the maximal concentration term and [Ca] is determined in the supernatant (by AAS and with arsenazo III).

As seen in Fig. 2, the data fit using Eq. (10) faces the problem of large data scatter, inherent in the method of vesicle preparation and handling as a pellet and the supernatant. Nevertheless, the fit yields reliably $K^0_{Ca} = 15 \pm 5$ μM and $[Ca_b]^{max} = 170 \pm 20$ μM at $T = 293$ K (20 °C), 1 mM HEPES, pH 7.4.

For consistency check, two other methods, AAS and arsenazo III, have been used to determine the dissociation equilibrium constant K^0_{Ca} and $[Ca_b]^{max}$ in the pellet; here $[Ca_t]^{sup} = [Ca]$. See Fig. A2 of the Appendix. The data fit for the relation $[Ca_b] = [Ca_t] - [Ca]$ versus [Ca] yields the same values for K^0_{Ca} and $[Ca_b]^{max}$ as obtained from the spectrophotometric Ca^{2+}-titration of the vesicles.

If B for the binding of Ca^{2+} refers to 2 anionic PS molecules, the maximum concentration of the bound Ca^{2+} on the vesicle surface is $[Ca_b]^{max} = [Ca(PS)_2]^{max} = [PS_b]^{max}/2$; that is approximately equal to half the concentration of complex (or bound) PS on the vesicle membrane. With the total lipid concentration $[L_t] = 1$ mM, we obtain $[PS] = [L_t]/3 = 0.33$ mM. Since DNA-binding in the titration method occurs only on the outside monolayer of the vesicle bilayer, the head group concentration available for the DNA/Ca/PS complexation on the outside is $[PS]/2 = 0.165$ mM.

A survey of the binding of Ca^{2+}-ions to membrane surfaces, modelled by monolayers, bilayers and lipid vesicles, indicates largely different equilibrium constants. Note that apparent equilibrium constants are dependent on the ionic strength. In particular, when [NaCl] decreases from 100 mM to 10 mM, the apparent dissociation constant of the Ca/PS system decreases about two orders of magnitude [8,32]. See Table 1.

4.4. The binding of Ca^{2+} to DNA

4.4.1. The binding of Ca^{2+} to DNA in solution (without vesicles)

If the binding of Ca^{2+} to DNA (D) is specified as a dissociation reaction according to:

$$CaD \rightleftharpoons Ca + D, \tag{11}$$

the degree of Ca^{2+} binding to DNA in solution is defined as:

$$\beta_{CaD} = \frac{[CaD]}{[CaD]^{max}} = \frac{[Ca]}{[Ca] + K^0_{CaD}} \tag{12}$$

where K^0_{CaD} is the respective apparent equilibrium constant (Eq. (7)) and β_{CaD} is obtained from the absorbance ratio according to $\beta_{CaD} = \Delta A / \Delta A_0 = (A_0 - A)/(A_0 - A_{min})$ (Fig. 3).

Table 1
Apparent dissociation equilibrium constants of the binding of Ca^{2+} to lipids

K^0_{Ca}	Lipid composition	Buffer	Reference
0.07 μM (7 mN/m) 0.035 μM (32.4 mN/m)	PS (monolayer)	Distilled water, $T = 293$ K (20 °C)	[33]
6 μM	PS (bilayer, vesicles)	1 mM Ca^{2+}, $T = 293$ K (20 °C)	[9]
98 μM	PA/PS (1:5)	145 mM NaCl, pH 7.4, $T = 293$ K (20 °C)	[34]
100 μM	PA/PS (1:2)		
79 μM	PA/PS (4:5)		
85 μM	PC/PS		
83.3 mM	PS (vesicle)	100 mM NaCl, pH 7.5, $T = 293$ K (20 °C)	[8]
27.7 mM		10 mM NaCl, pH 7.5, $T = 293$ K (20 °C)	
28.6 mM	PS (vesicle)	100 mM NaCl, 2 mM L-histidine, 2 mM TES, pH 7.4, $T = 293$ K (20 °C)	[6]
265 μM	PS (vesicle)	100 mM NaCl, pH 7.4, $T = 293$ K (20 °C)	[7]
124 mM	PC/PE/PS (4:4:1) multilamellar liposomes	100 mM NaCl, 10 mM HEPES, pH 7.4, $T = 298$ K (25 °C)	[29]
1.8 ± 0.3 mM	Yeast cells	1 mM sorbitol, 1 mM Tris–HCl, pH 7.4 $T = 293$ K (20 °C)	[16]
39.5 mM	Neuroblastoma cells	Dulbecco's, Eagle's	[35]

Note that D represents two neighbouring phosphate residues or, formally, one base pair. Here, the maximum concentration $[CaD]^{max}$, of the CaD complex is approximated by $[CaD]^{max}=[D_t]$. The data (Fig. 3) are evaluated according to:

$$A - A_{min} = (A_0 - A_{min})\frac{K^0_{CaD}}{[Ca] + K^0_{CaD}} \quad (13)$$

with $A_0=0.422\pm0.002$ and $A_{min}=0.388\pm0.002$. K^0_{CaD} is calculated from the half-point at $\beta_{CaD}=0.5$, using:

$$K^0_{CaD} = [Ca]_{0.5} = [Ca_t]_{0.5} - [D_t]/2. \quad (14)$$

In the example shown in Fig. 3, $[Ca_t]_{0.5}=40\pm5$ μM and thus $K^0_{CaD}=24\pm5$ μM at $T=293$ K (20 °C), 1 mM HEPES, pH 7.4.

4.5. The binding of Ca^{2+} to DNA in the supernatant

In the presence of vesicles, the Ca^{2+}-binding to DNA is evaluated from the supernatant data. The equilibrium constant K^0_{CaD} is related to β_{CaD} with the specification $[CaD]^{max}=[D_t]^{sup}$; Eq. (12).

Graphically (Fig. 7), for a given total DNA concentration, $[D_t]^{sup}$, in the supernatant, the equilibrium constant K^0_{CaD} is determined from the half-points at $\beta_{CaD}=0.5$. See Eq. (A2) of the Appendix. There is another consistency check for the determination of K^0_{CaD} according to the relationship:

$$K^0_{CaD} = [Ca]\left(\frac{[D_t]^{sup}}{[Ca_t]^{sup} - [Ca]} - 1\right) \quad (15)$$

which is obtained from Eq. (12) by using $[CaD]^{max}=[D_t]^{sup}$ and mass conservation according to: $[CaD]=[Ca_t]^{sup}-[Ca]$. See Fig. A3 of the Appendix. The calculation yields $K^0_{CaD}=26\pm6$ μM, being close to $K^0_{CaD}=24\pm5$ μM from Fig. 3. Previous documentations of Ca/DNA dissociation equilibrium constants strongly vary. Apparent dissociation constants of $K_{CaD}=0.5$ mM and $K_{CaD}=0.3$ mM have been reported for DNA from *Micrococcus lysodeikticus* in 50 mM electrolyte solution at 23 °C [12]. For Mg^{2+}, the low value $K_{MgD}=1.6$ μM refers to the low ionic strength of 1 mM [13] and is thus comparable with $K^0_{CaD}=24\pm5$ μM for Ca^{2+} found here. It is recalled that generally the apparent equilibrium constant depends on the type of divalent ion and the ionic strength.

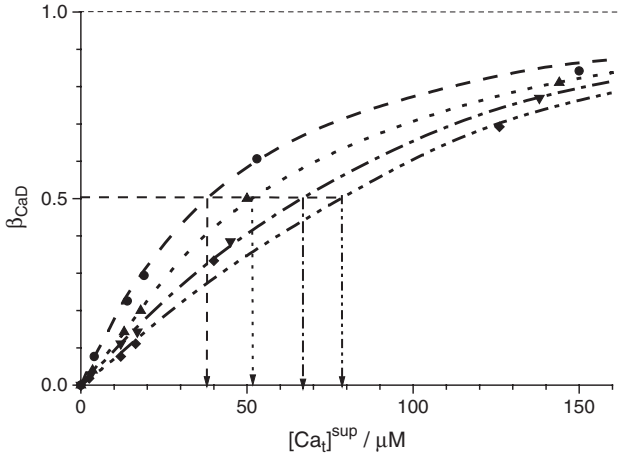

Fig. 7. The degree of binding β_{CaD} in the supernatant, calculated with Eq. (12) (or (A2) of the Appendix) at $[D_t]$/μM (bp)= (●) 35.5, (▲) 71, (▼) 107 and (♦) 143. $[D_t]$ refers to the total concentration of DNA in the vesicle suspension. The arrows represent $[Ca_t]^{sup}$ at β_{CaD}=0.5.

Note that the data for the Ca^{2+} binding to vesicles (Fig. 2) and for the DNA binding to vesicles (Fig. 3) both refer to the suspension (no precipitation by centrifugation). The data in Fig. 4 refer separately to the Ca^{2+}-binding to DNA in the supernatant and, on the other hand, to Ca^{2+}-binding to DNA and vesicles in the pellet. Remarkably, suspension data, supernatant data and pellet data lead to the same K-values within the margin of error. Therefore, as already reflected in the spectrophotometric data, there is no sign of Ca^{2+}-induced aggregation neither of DNA nor of vesicles, in the range of $[Ca_t]\leq1$ mM used here. Naturally, there is vesicle aggregation in the pellet.

4.6. Overall DNA-binding to sites B on the vesicle and to the complex CaB

It is appropriate to describe the overall binding of DNA by the overall reaction scheme:

$$D + (B + CaB) \rightleftharpoons (DB + DCaB) \quad (16)$$

where the Ca^{2+}-dependent overall dissociation equilibrium constant is given by:

$$\overline{K'_D}^{(Ca)} = [D]\cdot\frac{[B] + [CaB]}{[DB] + [DCaB]} = [D]\cdot\frac{1-\overline{\beta_D}}{\overline{\beta_D}} = [D]_{\overline{\beta_D}=0.5} \quad (17)$$

and the overall degree of binding $\overline{\beta_D}$ refers to:

$$\overline{\beta_D} = \frac{[DB] + [DCaB]}{([DB] + [DCaB])^{max}} = \frac{[D_b]}{[D_b]^{max}} = \frac{[D]}{[D] + \overline{K'_D}^{(Ca)}} \quad (18)$$

where $[D_b]^{max}=[B^D_t]$ is the total concentration of B sites available for the DNA-binding on the vesicle surface. The concentration $[D]$ of free DNA in the supernatant decreases with increasing concentration [Ca] of free Ca^{2+} in the supernatant, as expected in line with the relationship:

$$[D] = [D_t]^{sup}\cdot\frac{K^0_{CaD}}{[Ca] + K^0_{CaD}} \quad (19)$$

obtained by substitution of $[CaD]^{max}=[D_t]^{sup}$ and $[CaD]=[D_t]^{sup}-[D]$ in Eq. (12). See Fig. A4 of the Appendix. The

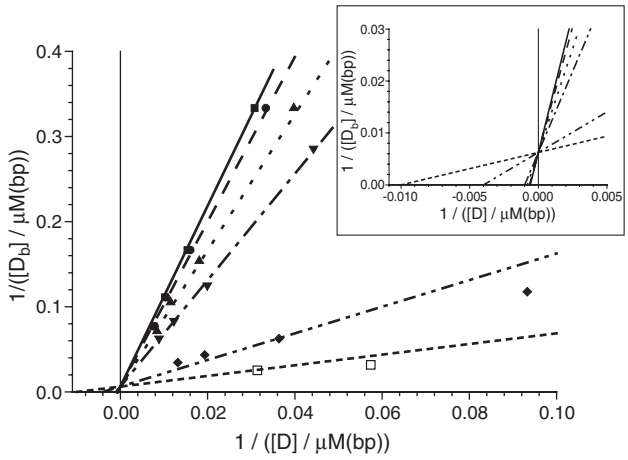

Fig. 8. The graphical determination of $[D_b]^{max}$ and $\overline{K'_D}^{(Ca)}$ from the double-reciprocal relationship according to Eq. (23) for $[Ca_t]$/μM=(■) 0, (●) 25, (▲) 75, (▼) 100, (♦) 200 and (□) 300. The insert shows the enlarged intercept and the abscissa intersections.

overall equilibrium constant $\overline{K'_D}^{(Ca)}$ can also be expressed as:

$$\overline{K'_D}^{(Ca)} = K'_D \cdot \frac{[Ca] + K^0_{Ca}}{[Ca] + K'_{Ca}}. \quad (20)$$

Eq. (20) is derived from Eq. (17); see Eq. (A4) of the appendix. In the case $[Ca_t]=0$ (full line in Fig. 8), the reaction scheme (16) reduces to:

$$D + B \rightleftharpoons DB \quad (21)$$

and Eq. (20) yields:

$$\overline{K'_D}^{(Ca)} = K'_D \cdot K^0_{Ca}/K'_{Ca} = K^0_D, \quad (22)$$

where K^0_D (=[D] [B]/[DB]) refers to the adsorption of DNA to lipid surfaces in the absence of added Ca^{2+}-ions [36]. Rearranging now Eq. (18) as a double-reciprocal relationship we obtain:

$$\frac{1}{[D_b]} = \frac{1}{[B^D_t]} \cdot \left(1 + \frac{\overline{K'_D}^{(Ca)}}{[D]}\right), \quad (23)$$

for different $[Ca_t]$ of the suspension (Fig. 8).

In the case of DNA binding in the absence of Ca^{2+}-ions ($[Ca_t]=0$), we obtain the solid line in Fig. 8. The intercept yields the common value $[B^D_t]=160\pm20$ μM and the abscissa yields the various numerical values of $\overline{K'_D}^{(Ca)}$. The concentration $[B^D_t]$ of binding sites for DNA is approximately equal to the maximum concentration, $[Ca_b]^{max}/2$, represented by the head group concentration [PS]/2 of PS available at the outer vesicle surface. For, $\overline{K'_D}^{(Ca)} = [D]_{\overline{\beta_D}=0.5}$, at each value of $[Ca_t]$ and at the half-point of bound DNA, $[D_b]_{0.5}=[D_b]^{max}/2=[B^D_t]/2=80$ μM, we obtain the respective value for the DNA-binding (data not shown) and a value $[Ca]_{0.5}$ of the free Ca concentration at $\overline{\beta_D}=0.5$ according to:

$$[Ca]_{0.5} = K^0_{CaD}\left([D_t]^{sup}_{0.5}/[D]_{0.5} - 1\right). \quad (24)$$

Again, Eq. (24) is obtained by substitution of $[CaD]^{max}=[D_t]^{sup}$ and $[CaD]=[D_t]^{sup}-[D]$ into Eq. (12). In Fig. 9, it is seen that $\overline{K'_D}^{(Ca)}$ decreases with increasing half-point concentration $[Ca]_{0.5}$, according to Eq. (20) with $K^0_{Ca} \gg K'_{Ca}$. At $[Ca]=0$, $\overline{K'_D}^{(Ca)}=K'_D-K^0_{Ca}/K'_{Ca}=K^0_D$ and at $[Ca] \gg K^0_{Ca}$, and $[Ca] \gg K'_{Ca}$, we have $\overline{K'_D}^{(Ca)}=K'_D$. The data fit with Eq. (20) yields $K^0_D=1.7\pm0.1$ mM (bp) and $K'_D=85\pm15$ μM (bp) at $T=293$ K (20 °C), 1 mM HEPES, pH 7.4. The results are in line with $K^0_{Ca}=24\pm5$ μM, being indeed larger than $K^0_{Ca}=0.75\pm0.25$ μM; see below. As a further consistency check, the values of $\overline{K'_D}^{(Ca)}$ are calculated for each value of $[D_b]$, $[D_t]^{sup}$ and [Ca]. Introducing Eq. (19) into Eq. (23), rearrangement yields:

$$\overline{K'_D}^{(Ca)} = \left(\frac{[B^D_t]}{[D_b]} - 1\right) \cdot \frac{[D_t]^{sup} \cdot K^0_{CaD}}{[Ca] + K^0_{CaD}}. \quad (25)$$

Data fit analogous to the data fit with Eq. (20) yields $K'_D=85\pm15$ μM (bp) and K^0_D 1.7 ± 0.1 mM (bp). See Fig. A5 of the Appendix. The results are consistent with those obtained from Eq. (23).

4.7. Overall Ca^{2+}-binding to sites B on the vesicle and to the complex DB

Similar to the overall reaction scheme (16) for DNA-binding, we express the overall binding according to:

$$Ca + (B + DB) \rightleftharpoons (CaB + DCaB(DCa)) \quad (26)$$

where the DNA-dependent overall equilibrium constant is defined by:

$$\overline{K'_{Ca}}^{(D)} = [Ca] \cdot \frac{[B] + [DB]}{[CaB] + [DCaB(DCa)]} = [Ca] \cdot \frac{1 - \overline{\beta_{Ca}}}{\overline{\beta_{Ca}}} = [Ca]_{\overline{\beta_{Ca}}=0.5}. \quad (27)$$

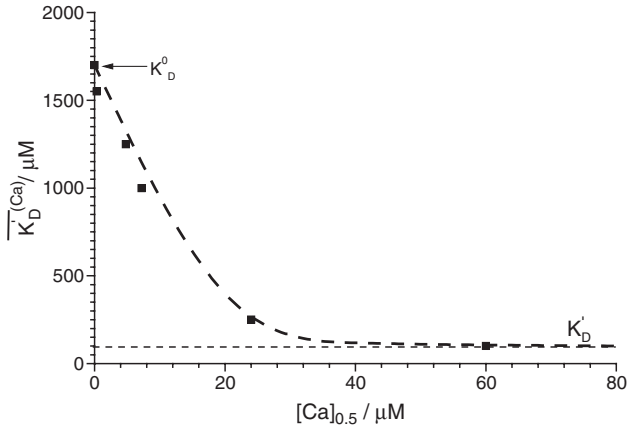

Fig. 9. The overall equilibrium constants $\overline{K'_D}^{(Ca)}$ obtained from the abscissa intercepts in Fig. 8. The data fit with Eq. (20) yields $K^0_D=1.7\pm0.1$ mM (bp) and $K'_D=85\pm15$ μM (bp) at $T=293$ K (20 °C), 1 mM HEPES, pH 7.4.

The overall degree of Ca^{2+}-binding refers to:

$$\overline{\beta_{Ca}} = \frac{[CaB] + [DCaB(DCa)]}{([CaB] + [DCaB(DCa)])^{max}} = \frac{[Ca_b]}{[Ca_b(D)]^{max}} = \frac{[Ca]}{[Ca] + \overline{K'_{Ca}}^{(D)}}. \quad (28)$$

The part (DCa) in the complex DCaB(DCa) accounts for the Ca^{2+}-binding to those base pairs of DNA which are not yet bridged by Ca^{2+}-ions to the lipid surface. Consistent with expectations, the concentration of bound Ca^{2+} in the pellet $[Ca_b]=[CaB]+[DCaB(DCa)]$ increases with increasing $[Ca_t]$ and $[D_t]$, respectively (Fig. 10).

Trivially at $[D]=0$, $[Ca_b]=[CaB]$. With increasing $[D_t]$, $[Ca_b]$ in the complex $[DCaB(DCa)]$ increases first due to Ca^{2+}-bridging D and B as complex DCaB and then additionally due to further Ca^{2+}-binding to the DNA (as DCa) not yet bridged to B-sites as DCaB, reducing the amount of CaB.

Parallel to the formalism used for the overall DNA-binding, the overall equilibrium constant $\overline{K'_{Ca}}^{(D)}$ for the Ca^{2+}-binding is given by:

$$\overline{K'_{Ca}}^{(D)} = K'_{Ca} \cdot \frac{[D] + K^0_D}{[D] + K'_D}. \quad (29)$$

Eq. (29) is derived from Eq. (27); see Eq. (A5) of the Appendix. From Eq. (28) we obtain the double-reciprocal relationship:

$$\frac{1}{[Ca_b]} = \frac{1}{[Ca_b(D)]^{max}} \left(1 + \overline{K'_{Ca}}^{(D)} \frac{1}{[Ca]}\right). \quad (30)$$

Using Eq. (30) at different $[D_t]$, the intercepts yield $[Ca_b\ (D)]^{max}$ and $\overline{K'_{Ca}}^{(D)}$, respectively (Fig. 11). For each

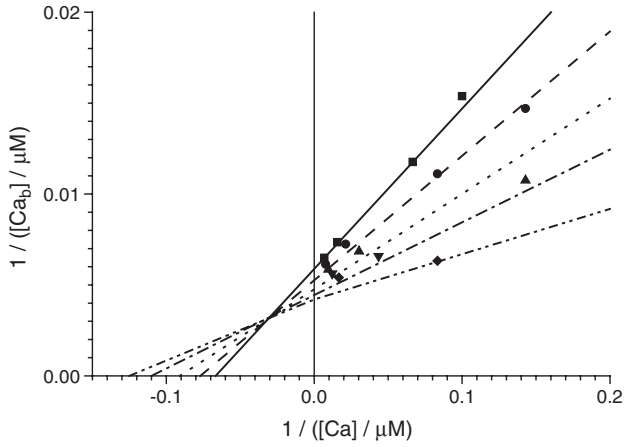

Fig. 11. Determination of $\overline{K'_{Ca}}^{(D)}$ and $[Ca_b]^{max}$ from the double-reciprocal relationship Eq. (30) for $[D_t]$/µM (bp)= (■) 0, (●) 35.5, (▲) 71, (▼) 107 and (♦) 143. (The intersection point is at: $1/[Ca]_i = -0.0032\ \mu M^{-1}$ and $1/[Ca_b]_i = 0.0032\ \mu M^{-1}$ (see the Appendix).

$\overline{K'_{Ca}}^{(D)}$ at a given $[D_t]$ there is a half-point concentration $[Ca_b]_{0.5}=[Ca_b(D)]^{max}/2$ at given $[Ca_t]_{0.5}$, $[Ca]_{0.5}$ and $[D]_{0.5}$, respectively. It is seen that the values of $\overline{K'_{Ca}}^{(D)}$ are equal to those of $[Ca]_{0.5}$, within the error margin. The coordinates of the intersection point are given by Eq. (A6) of the Appendix.

As seen in Fig. 12, the overall equilibrium constant $\overline{K'_{Ca}}^{(D)}$ decreases with increasing half-point concentration $[D]_{0.5}$ according to Eq. (29) with $K^0_D \gg K'_D$. At $[D]=0$, $\overline{K'_{Ca}}^{(D)} = K^0_D \cdot K'_{Ca}/K'_D = K^0_{Ca}$ and at $[D] \gg [D_t]$ (saturation) we obtain $\overline{K'_{Ca}}^{(D)} = K'_{Ca}$. The data fit with Eq. (29) yields $K^0_{Ca}=15\pm5$ µM and $K'_{Ca}=0.75\pm0.25$ µM at $T=293$ K (20 °C), 1 mM HEPES, pH 7.4, confirming that indeed $K^0_{Ca} \gg K'_{Ca}$.

The maximum concentration $[Ca_b(D)]^{max}$ of Ca^{2+} bound to the outer vesicle surface in the presence of bound DNA

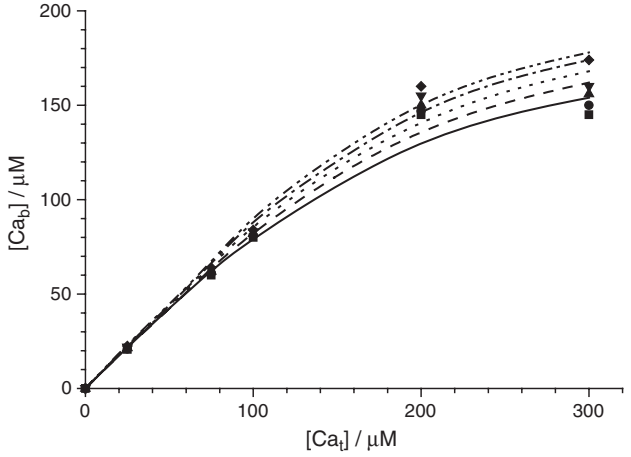

Fig. 10. The concentration $[Ca_b]=[CaB]+[DCaB(DCa)]=[Ca_t]-[Ca_t]^{sup}$ of bound Ca^{2+} in the pellet for $[D_t]$/µM (bp)=(■) 0, (●) 35.5, (▲) 71, (▼) 107 and (♦) 143 versus $[Ca_t]$. Note, that $[D_t]$ refers to the concentration of DNA in the vesicle suspension.

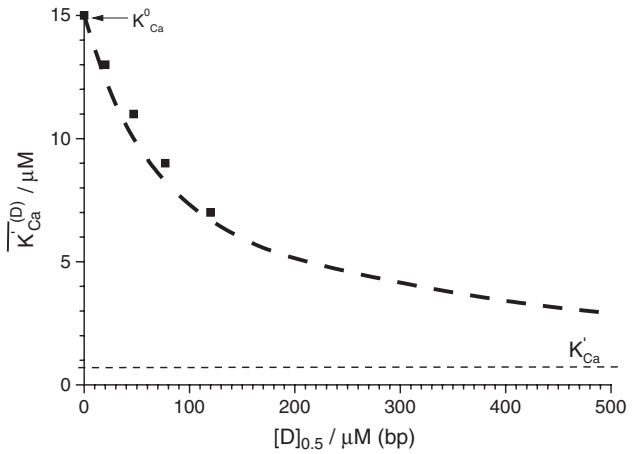

Fig. 12. The overall equilibrium constants $\overline{K'_{Ca}}^{(D)}$ determined with Eq. (30). Data fit with Eq. (29) yields $K^0_{Ca}=15\pm5$ µM and $K'_{Ca}=0.75\pm0.25$ µM at $T=293$ K (20 °C), 1 mM HEPES, pH 7.4.

Table 2
The apparent dissociation equilibrium constants for the system DNA, Ca^{2+}-ions, lipid vesicle surface (PS) in 1 mM HEPES, pH 7.4, T=293 K (20 °C)

Binary complexes	Ternary complexes
K^0_{Ca}=15±5 μM	K'_{Ca}=0.75±0.25 μM
K^0_{CaD}=24±5 μM	K'_{CaD}=53±10 μM (bp)
K^0_D=1.7±0.1 mM (bp)	K'_D=85±15 μM (bp)

increases with increasing total concentration of DNA according to mass conservation:

$$[\mathrm{Ca_b}(D)]^{\max} = [\mathrm{Ca}B]^{\min} + [D\mathrm{Ca}B(D\mathrm{Ca})]^{\max} = [\mathrm{Ca}B]^{\max} + [D_t] - [D\mathrm{Ca}B]. \quad (31)$$

Note that $[\mathrm{DCaB}]^{\max}+[\mathrm{DCa}]^{\max}=[D_t]$ and $[\mathrm{CaB}]^{\min}=[\mathrm{CaB}]^{\max}-[\mathrm{DCaB}]$. See Fig. A6 of the Appendix.

As a further consistency check, $\overline{K'_{Ca}}^{(D)}$ is calculated using the values for $[D]$, $[\mathrm{Ca_t}]^{\mathrm{sup}}$, $[\mathrm{Ca_b}]$ and $[\mathrm{Ca_b}(D)]^{\max}$. Introducing Eq. (12) into Eq. (30) and rearranging yields:

$$\overline{K'_{Ca}}^{(D)} = \left(\frac{[\mathrm{Ca_b}(D)]^{\max}}{[\mathrm{Ca_b}]} - 1\right)\cdot\frac{[\mathrm{Ca_t}]^{\mathrm{sup}}\cdot K^0_{CaD}}{[D]+K^0_{CaD}}. \quad (32)$$

Data fit with Eq. (29) yields K^0_{Ca}=15±5 μM and K'_{Ca}=0.75±0.25 μM at T=293 K (20 °C), 1 mM HEPES, pH 7.4. See Fig. A7 of the Appendix. These results are consistent with those obtained with Eq. (30).

The equilibrium constant K'_{CaD} is calculated using the definitions of the apparent equilibrium constants in Eqs. (7) and (8), respectively; according to:

$$K'_{CaD} = \frac{[\mathrm{Ca}D]\cdot[B]}{[D\mathrm{Ca}B]} = \frac{[D]\cdot[\mathrm{Ca}B]}{[D\mathrm{Ca}B]}\cdot\frac{[\mathrm{Ca}]\cdot[B]/[\mathrm{Ca}B]}{[\mathrm{Ca}]\cdot[D]/[\mathrm{Ca}D]} = K'_D\cdot\frac{K^0_{Ca}}{K^0_{CaD}}, \quad (33)$$

Eq. (33) yields K'_{CaD}=53±10 μM (bp) at T=293 K (20 °C), 1 mM HEPES, pH 7.4.

As seen in Table 2, the dissociation equilibrium constants for the binary complexes are greater as the respective constants for the ternary complexes, i.e. the ternary complexes are more stable than the binary complexes.

5. Conclusions

Using centrifugation, atom absorption spectrometry and arsenazo III absorbance, the binding of DNA at lipid vesicle surface mediated by Ca^{2+}-ions is measured. The independent spectroscopic measurements permit the determination of the apparent dissociation equilibrium constants for the binary complexes: Ca/lipid vesicles, Ca/DNA and DNA/lipid vesicles and for the various processes leading to the ternary complex DNA/Ca/lipid vesicles. The thermodynamic formalism has been developed such that the experimental overall dissociation equilibrium constants for the binding of Ca^{2+} and DNA to the vesicle surface, respectively, appear as combinations of the individual binary equilibrium constants. The thermodynamic stabilities of the respective ternary complexes are two orders of magnitude greater than that of the binary complexes: Ca/lipids and DNA/lipids.

The knowledge of the equilibrium constants for the adsorption of DNA and the binding of DNA to the vesicle surface, provide the basis for choosing the respective optimal concentrations, to optimize the conditions of the adsorption for the direct electrotransfer of gene-DNA into biological cells and tissue.

Acknowledgments

We gratefully acknowledge support of the Fonds Chemie, Frankfurt, the Ministry MSWF of the Land NRW for Grant Elminos, the European Union (Brüssel) for Grant QLK3-CT-1999-00484 and the Deutsche Forschungsgemeinschaft for Grants Ne227/9-3 and 9-4 to E.N.

Appendix A

A.1. The binding of Ca^{2+} to DNA in the supernatant

In the presence of vesicles, the degree β_{CaD} of Ca^{2+} binding to DNA in the supernatant is given by:

$$\beta_{CaD} = \frac{[\mathrm{Ca}D]}{[\mathrm{Ca}D]^{\max}} = \frac{[\mathrm{Ca}D]}{[D_t]^{\mathrm{sup}}} = \frac{[\mathrm{Ca}]}{[\mathrm{Ca}]+K^0_{CaD}} \quad (A1)$$

where the relation $[D_t]^{\mathrm{sup}}=[\mathrm{Ca}D]^{\max}$ holds.

Note that $K^0_{CaD}=[\mathrm{Ca}]\cdot[\mathrm{D}]/[\mathrm{CaD}]=[\mathrm{Ca}]\cdot(1-\beta_{CaD})/\beta_{CaD}$; hence $\beta_{CaD}\cdot(K^0_{CaD}+[\mathrm{Ca}])=[\mathrm{Ca}]$ yielding Eq. (A1)

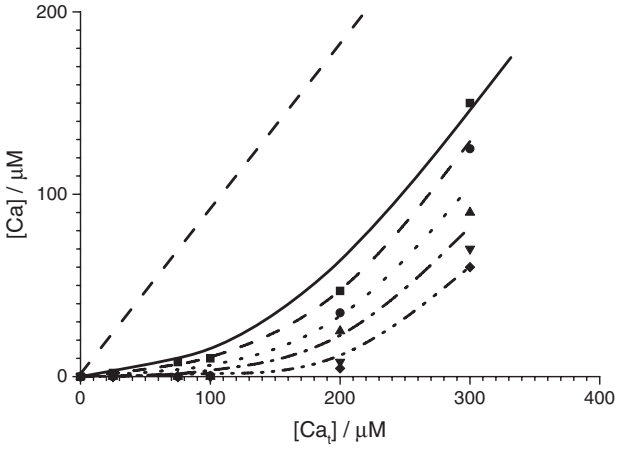

Fig. A1. Ca^{2+}-binding isotherms for different DNA concentrations: $[D_t]$/μM (bp): (■) 0, (●) 35.5, (▲) 71, (▼) 107 and (♦) 143; from top to bottom. The data are fitted with Eq. (12) of the text, where $[\mathrm{Ca_t}]=[\mathrm{Ca_b}]+[\mathrm{Ca_t}]^{\mathrm{sup}}$. The straight dashed line represents the case without vesicles and without DNA for which $[\mathrm{Ca}]=[\mathrm{Ca_t}]=[\mathrm{Ca_t}]^{\mathrm{sup}}$.

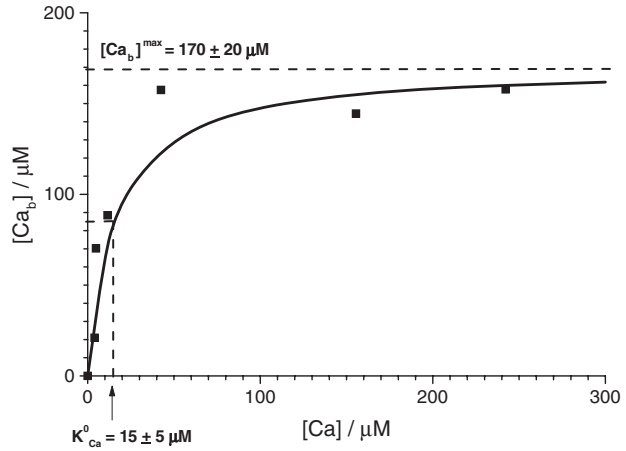

Fig. A2. Ca^{2+}-binding isotherms in the absence of DNA, $[Ca_b]=[Ca_t]-[Ca]$, in the pellet as a function of [Ca] in the supernatant. The data points represent mean values of two measurements of Ca^{2+} in the supernatant by arsenazo III-absorption and atomic absorption spectroscopy. Here, $[Ca]=[Ca_t]^{sup}$. Data fit with Eq. (10) of the text yields the equilibrium constant $K^0_{Ca}=15\pm5$ µM and $[Ca_b]^{max}=170\pm20$ µM at T= 293 K (20 °C), 1 mM HEPES, pH 7.4.

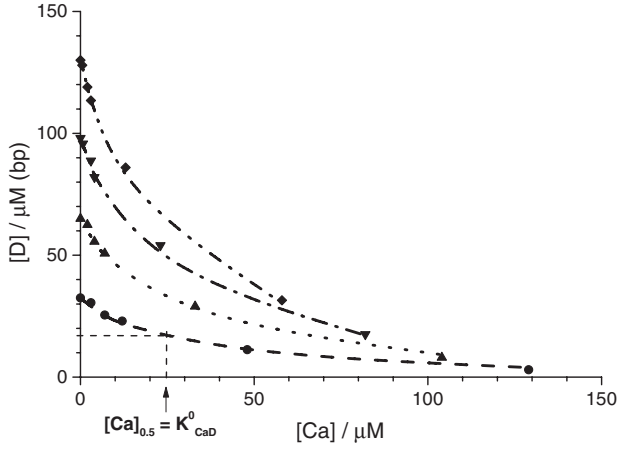

Fig. A4. The relationship between $[D]=[Ca]+[D_t]^{sup}-[Ca_t]^{sup}$ and [Ca] for $[D_t]$/µM (bp)= (●) 35.5, (▲) 71, (▼) 107 and (♦) 143. $[D_t]$ refers to the concentration of DNA in the vesicle suspension. The data are fitted with the Eq. (19) of the text.

or the relationship: $[CaD]=[D_t]^{sup}\cdot[Ca]/([Ca]+K^0_{CaD})$. Insertion into $[Ca_t]^{sup}=[Ca]+[CaD]$ yields: $[Ca]=[Ca_t]^{sup}-[D_t]^{sup}\cdot[Ca]/([Ca]+K^0_{CaD})$.

The equilibrium constant $K^0_{CaD}=[Ca]_{\beta_{CaD}=0.5}$ in the presence of vesicles is related to the total Ca^{2+} concentration $[Ca_t]$ of pellet and supernatant and the total DNA concentration $[D_t]^{sup}$ in the supernatant by:

$$[Ca_t]^{sup}_{0.5}=K^0_{CaD}+[D_t]^{sup}/2. \quad (A2)$$

A.2. Determination of [Ca] with Ar

Similar to Eq. (A2), the equilibrium constant $K_{CaAr}=3.5\pm0.5$ µM is obtained from the midpoint (half-point) of the relation ΔA_{602} vs. log ($[Ca_t]$/mM) (data not shown) according to:

$$K_{CaAr}=[Ca_t]_{\beta_{CaAr}=0.5}-[Ar_t]/2, \quad (A3)$$

where $[Ca_t]_{\beta_{CaAr}=0.5}$ refers to $\Delta A_{602}=\Delta A^{max}_{602}/2$ and $\Delta A_{602}=A_{602}-A^0_{602}$, and $A^0_{602}=\varepsilon_{Ar}\cdot d\cdot[Ar_t]$ at $[Ca]=0$ (experimentally realised with 1 mM EDTA).

A.3. Overall DNA-binding to sites B on the vesicle surface and to complex CaB

Using the definitions of the apparent equilibrium dissociation constants in Eqs. (7) and (8), respectively, of

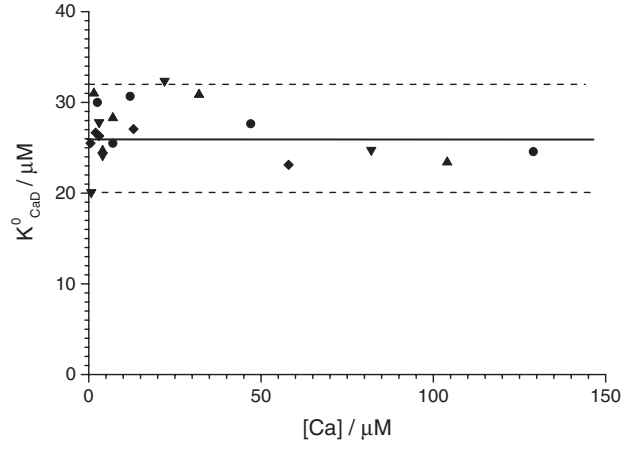

Fig. A3. The equilibrium constant K^0_{CaD} calculated with Eq. (15) for $[D_t]$/µM (bp)= (●) 35.5, (▲) 71, (▼) 107 and (♦) 143 as a function of [Ca]. The straight thick line represents the mean of $K^0_{CaD}=26\pm6$ µM.

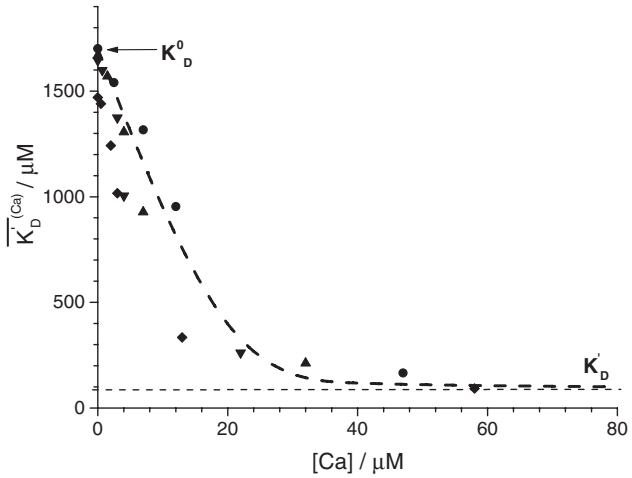

Fig. A5. The overall binding constant $\overline{K'^{(D)}_{Ca}}$ calculated with Eq. (25) for $[D_t]$/µM (bp)= (●) 35.5, (▲) 71, (▼) 107 and (♦) 143 as a function of [Ca]. $[D_t]$ refers to the total concentration of DNA in the vesicle suspensions. The data fit with Eq. (20) yields $K'_D=85\pm15$ µM (bp) and $K^0_D=1.7\pm0.1$ mM (bp) at T= 293 K (20^0 C), 1 mM HEPES, pH 7.4.

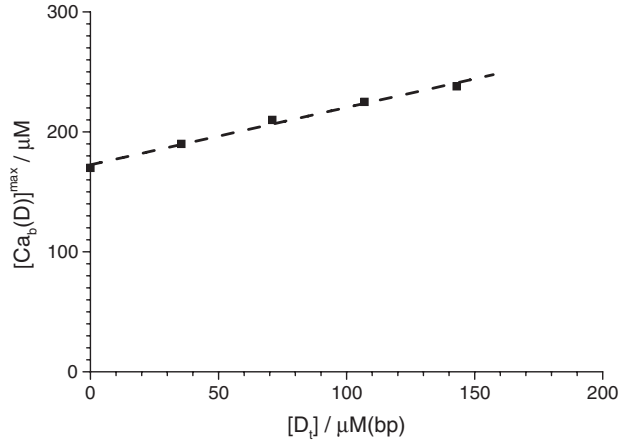

Fig. A6. The total concentrations of sites available for Ca^{2+}-binding on the vesicle surface $[Ca_b(D)]^{max}=[CaB]^{max}+[D_t]-[DCaB]$. $[Ca_b(D)]^{max}$ increases linearly with $[D_t]$ due to the increased number of sites D(bp) not involved in the ternary complex DCaB, but binding Ca^{2+}-ions as CaD within the DNA partially attached to the lipid surface.

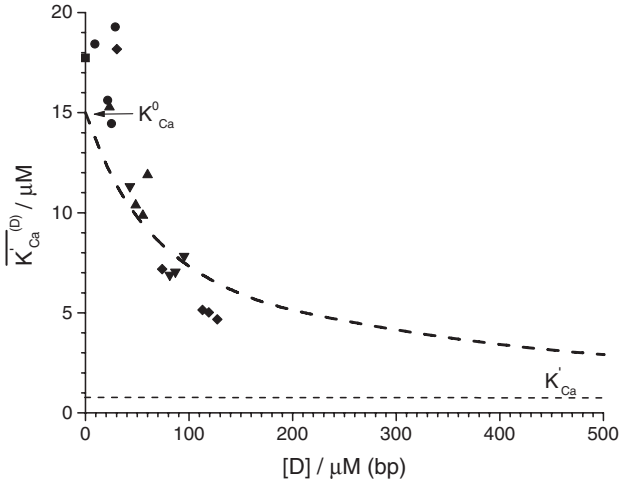

Fig. A7. The overall equilibrium constants $\overline{K'_{Ca}}^{(D)}$ as a function of $[D]$ calculated with Eq. (32) of the text for $[D_t]$/μM (bp)= (■) 0, (●) 35.5, (▲) 71, (▼) 107 and (♦) 143. Data fit with Eq. (29) yields $K^0_{Ca}=15\pm5$ μM and $K'_{Ca}=0.75\pm0.25$ μM at $T=293$ K (20 °C), 1 mM HEPES, pH 7.4.

the main text, the overall equilibrium constant for the Ca^{2+}-dependent binding of DNA is defined as:

$$\begin{aligned}\overline{K'_D}^{(Ca)} &= [D]\cdot\frac{[B]+[CaB]}{[DB]+[DCaB]}\\ &= [D]\cdot\frac{[B]\cdot(1+[CaB]/[B])}{[DB]\cdot(1+[DCaB]/[DB])}\\ &= K^0_D\cdot\frac{1+[Ca]/K^0_{Ca}}{1+[Ca]/K'_{Ca}}\\ &= K^0_D\cdot\frac{K'_{Ca}}{K^0_{Ca}}\cdot\frac{[Ca]+K^0_{Ca}}{[Ca]+K'_{Ca}} = K'_D\cdot\frac{[Ca]+K^0_{Ca}}{[Ca]+K'_{Ca}}\end{aligned} \quad (A4)$$

where the relation $K^0_D/K^0_{Ca}=K'_D/K'_{Ca}$ of the cyclic scheme (Fig. 7) is used. See Eq. (20) of the main text.

A.4. Overall Ca^{2+}-binding to sites B on the vesicle surface and to complex DB

The overall equilibrium constant for the DNA-dependent binding of Ca^{2+} according to scheme (26) is given by:

$$\begin{aligned}\overline{K'_{Ca}}^{(D)} &= [Ca]\cdot\frac{[B]+[DB]}{[CaB]+[DCaB(DCa)]}\\ &= [Ca]\cdot\frac{[DB]\cdot(1+[B]/[DB])}{[DCaB(DCa)]\cdot(1+[CaB]/[DCaB(DCa)])}\\ &= K'_{Ca}\cdot\frac{1+K^0_D/[D]}{1+K'_D/[D]} = K'_{Ca}\cdot\frac{[D]+K^0_D}{[D]+K'_D}\end{aligned} \quad (A5)$$

where the relation $K'_{Ca}=K'_D\cdot K^0_{Ca}/K^0_D$ is inherent; see Eq. (29) of the main text.

The intersection point in Fig. 11 is obtained from Eq. (30) of the main text for $[D_t]\neq0$ and $[D_t]=0$, where $1/[Ca_b]=(1/[Ca_b]^{max})(1+K^0_{Ca}/[Ca])$. The coordinates $1/[Ca]_i$ and $1/[Ca_b]_i$ of the intersection point are given by:

$$\frac{1}{[Ca]_i} = -\frac{[Ca_b(D)]^{max}-[Ca_b]^{max}}{[Ca_b(D)]^{max}\cdot K^0_{Ca}-[Ca_b]^{max}\cdot\overline{K'_{Ca}}^{(D)}}$$

$$\frac{1}{[Ca_b]_i} = \frac{K^0_{Ca}-\overline{K'_{Ca}}^{(D)}}{[Ca_b(D)]^{max}\cdot K^0_{Ca}-[Ca_b]^{max}\cdot\overline{K'_{Ca}}^{(D)}} \quad (A6)$$

In Fig. 11, we see that $1/[Ca]_i=-0.03$ μM^{-1} and $1/[Ca_b]_i=0.0032$ μM^{-1}. Figs. A1–A7.

References

[1] L.M. Mir, M.F. Bureau, J. Gehl, R. Rangara, D. Rouy, J.-M. Caillaud, P. Delaere, D. Branellec, B. Schwartz, D. Scherman, High-efficiency gene transfer into skeletal muscle mediated by electric pulses, Proc. Natl. Acad. Sci. U. S. A. 96 (1999) 4262–4267.
[2] E. Neumann, M. Schaefer-Ridder, Y. Wang, P.H. Hofschneider, Gene transfer into mouse lyoma cells by electroporation in high electric fields, EMBO J. 1 (1982) 841–845.
[3] U. Pliquett, R. Elez, A. Piiper, E. Neumann, Electroporation of subcutaneous mouse tumors by rectangular and trapezium high voltage pulses, Bioelectrochemistry 62 (2004) 83–93.
[4] L.M. Mir, S. Orlowski, J. Belehradek Jr., J. Teissie, M.P. Rols, G. Sersa, D. Miklavcic, R. Gilbert, R. Heller, Biomedical applications of electric pulses with special emphasis on antitumor electrochemotherapy, Bioelectrochem. Bioenerg. 38 (1995) 203–207.
[5] R. Elez, A. Piiper, B. Kronenberger, M. Kock, M. Brendel, E. Hermann, U. Pliquett, E. Neumann, S. Zeuzem, Tumor regression by combination antisense therapy against Plk1 and Bcl-2, Oncogene 22 (2003) 69–80.
[6] C. Newton, W. Pangborn, S. Nir, D. Papahadjopoulos, Specificity of Ca^{2+} and Mg^{2+} binding to phosphatidylserine vesicles and resultant

phase changes of bilayer membrane structure, Biochim. Biophys. Acta 506 (1978) 281–287.
[7] A. Portis, C. Newton, W. Pangborn, D. Papahadjopoulos, Studies of the mechanism of membrane fusion: evidence for an intermembrane Ca^{2+}-phospholipid complex, synergism with Mg^{2+}, and inhibition by spectrin, Biochemistry 18 (1979) 780–790.
[8] S. McLaughlin, N. Murline, T. Gresalfi, G. Vaio, A. McLaughlin, Adsorption of divalent cations to bilayer membranes containing phosphatidyserine, J. Gen. Physiol. 77 (1981) 445–473.
[9] J. Bentz, S. Nir, Cation binding to membranes: competition between mono-, di- and trivalent cations, Bull. Math. Biol. 42 (1980) 191–220.
[10] A.M.I. Lam, P.R. Cullis, Calcium enhances the transfection potency of plasmid DNA-cationic liposome complexes, Biochim. Biophys. Acta 1463 (2000) 279–290.
[11] D.P. Kharakoz, R.S. Khusainova, A.V. Gorelov, K.A. Dowson, Stoichiometry of dipalmitoylphosphatidylcholine-DNA interaction in the presence of Ca^{2+}: a temperature-scanning ultrasonic study, FEBS Lett. 446 (1999) 27–29.
[12] J.T. Shapiro, B.S. Stannard, G. Felsenfeld, The binding of small cations to deoxyribonucleic acid. Nucleotide specificity, Biochemistry 8 (1969) 3233–3241.
[13] R.M. Clement, J. Sturm, M.P. Daune, Interaction of metallic cations with DNA VI. Specific binding of Mg^{2+} and Mn^{2+}, Biopolymers 12 (1973) 405–421.
[14] N. Korolev, A.P. Lyubartsev, A. Ruprecht, L. Nordenskiöld, Competitive binding of Mg^{2+}, Ca^{2+}, Na^{+} and K^{+} ions to DNA in oriented DNA fibers: experimental and Monte Carlo simulation results, Biophys. J. 77 (1999) 2736–2749.
[15] E. Süleymanoglu, A nanoscale polynucleotide-neutral liposome self-assemblies formulated for therapeutic gene delivery, Electron. J. Biomed. 2 (2) (2004).
[16] E. Neumann, S. Kakorin, I. Tsoneva, B. Nikolova, T. Tomov, Calcium-mediated DNA adsorption to yeast cells and kinetics of cell transformation by electroporation, Biophys. J. 71 (1996) 868–877.
[17] N. Stoicheva, I. Tsoneva, D.S. Dimitrov, I. Panaiotov, Kinetics of calcium-induced fusion of cell-size liposomes with monolayers in solutions of different osmolarity, Z. Naturforsch. 40c (1985) 92–96.
[18] F. Olson, C.A. Hunt, F.C. Szoka, W.J. Vail, D. Papahadjopoulos, Preparation of liposomes of defined size distribution by extrusion through polycarbonate membranes, Biochim. Biophys. Acta 557 (1979) 9–23.
[19] L.D. Mayer, M.J. Hope, P.R. Cullis, Vesicles of variable sizes produced by a rapid extrusion procedure, Biochim. Biophys. Acta 858 (1986) 161–168.
[20] A. Evilevitch, J.M. Gober, M. Phillips, C.M. Knobler, W.M. Gelbart, Measurements of DNA lengths remaining in a viral capsid after osmotically suppressed partial ejection, Biopys. J. 88 (2005) 751–756.
[21] V.A. Bloomfield, D.M. Crothers, I. Tinoco Jr., Molecular weight and long-range structure, in: Harper , Row (Eds.), Physical Chemistry of Nucleic Acids, New York, 1974, pp. 151–292.
[22] P.L. Dorogi, E. Neumann, Spectrophotometric determination of reaction stoichiometry and equilibrium constants of metallochromic indicators: II. The Ca^{2+}-Arsenazo III complexes, Biophys. Chem. 13 (1981) 125–131.
[23] J. Rosenberg, N. Duezguenes, C. Kayalar, Comparison of two liposome fusion assays monitoring the intermixing of aqueous contents and of membrane components, Biochim. Biophys. Acta 735 (1983) 173–180.
[24] Y.-C. Xu, H. Bremer, Winding of DNA helix by divalent metal ions, Nucleic Acids Res. 25 (1997) 4067–4071.
[25] V. Michaylova, P. Ilkova, Photometric determination of micro amounts of calcium with arsenazo III, Anal. Chim. Acta 53 (1971) 194–198.
[26] P.L. Dorogi, C.R. Rabl, E. Neumann, Kinetic scheme for Ca^{2+}-Arsenazo III interactions, Biochem. Biophys. Res. Commun. 111 (1983) 1027–1033.
[27] J.B. Willis, Determination of calcium and magnesium in urine by atomic absorption spectroscopy, Anal. Chem. 33 (1961) 556–559.
[28] D.J. Volsky, A. Loyter, Role of Ca^{2+} in virus-induced membrane fusion. Ca^{2+} accumulation and ultrastructural changes induced by Sendai virus in chicken erythrocytes, J. Cell Biol. 78 (1978) 465–479.
[29] D. Huster, K. Arnold, K. Gawrisch, Strength of Ca^{2+} binding to retinal lipid membranes: consequences for lipid organization, Biophys. J. 78 (2000) 3011–3018.
[30] C. Mangavel, R. Maget-Dana, P. Tauc, J.-C. Brochon, D. Sy, J.A. Reynaud, Structural investigations of basic amphipathic model peptides in the presence of lipid vesicles studied by circular dichroism, fluorescence, monolayer and modeling, Biochim. Biophys. Acta 1371 (1998) 265–283.
[31] T. Seimiya, S. Ohki, Ionic structure of phospholipid membranes and binding of calcium ions, Biochim. Biophys. Acta 298 (1973) 546–561.
[32] S. Nir, C. Newton, D. Papahadjopoulos, Binding of cations to phosphatidylserine vesicles, Bioelectrochem. Bioenerg. 5 (1978) 116–133.
[33] H. Hauser, D. Chapman, R.M.C. Dawson, Physical studies of phospholipids. XI. Ca^{2+} binding to monolayers of phosphatidylserine and phosphatidylinositol, Biochim. Biophys. Acta 183 (1969) 320–333.
[34] P.G. Barton, The influence of surface charge density of phosphatides on the binding of some cations, J. Biol. Chem. 243 (1968) 3884–3890.
[35] C. Xu, L.M. Loew, The effect of asymmetric surface potentials on the intramembrane electric field measured with voltage-sensitive dyes, Biophys. J. 84 (2003) 2768–2780.
[36] C. Fleck, R.R. Netz, H.H. von Grünberg, Poisson–Boltzmann theory for membranes with charged lipids and the pH-dependent interaction of a DNA molecule with a membrane, Biophys. J. 82 (2002) 76–92.

Glossary

Ar: arsenazo III
a_{coll}: collapse area per molecule
B: binding sites on the outside surface of the vesicles
β_{Ca}, β_{CaAr}, β_{CaD}: degree of Ca^{2+}-binding to vesicle surface, arsenazo III and DNA, respectively
$[Ca_t]$, $[D_t]$: total concentrations of Ca^{2+} and DNA, respectively
$[Ca]$, $[D]$: free concentrations of Ca^{2+} and DNA in the supernatant, respectively
$[Ca_t]^{sup}$, $[D_t]^{sup}$: total concentrations of Ca^{2+} and DNA in the supernatant, respectively
$[Ca_b]$, $[D_b]$: concentrations of bound Ca^{2+} and bound DNA in the pellet, respectively
$[Ca_b(D)]^{max}$: maximum concentration of sites available for Ca^{2+}-binding on the vesicle surface, including the bound DNA
$[D_b]^0$: concentration of DNA bound to the vesicle surface at $[Ca_t]=0$
K^0_{Ca}, K^0_D, K^0_{CaD}: dissociation equilibrium constants for the binary complexes
K'_{Ca}, K'_D, K'_{CaD}: dissociation equilibrium constants for the respective ternary complex formations
$\overline{K'^{(D)}_{Ca}}$, $\overline{K'^{(Ca)}_D}$: overall dissociation equilibrium constants for the respective Ca^{2+}- and DNA-binding
PS: phosphatidylserine
POPC: palmitoyl-oleoyl-phosphatidylcholine
PA: phosphoric acid
VET: vesicle extrusion technique